



Universiteit  
Leiden  
The Netherlands

## A mosaic variant in CTNNB1/ $\beta$ -catenin as a novel cause for osteopathia striata with cranial sclerosis

Huybrechts, Y.; Appelman-Dijkstra, N.M.; Steenackers, E.; Beylen, W. van; Mortier, G.; Hendrickx, G.; Hul, W. van

### Citation

Huybrechts, Y., Appelman-Dijkstra, N. M., Steenackers, E., Beylen, W. van, Mortier, G., Hendrickx, G., & Hul, W. van. (2024). A mosaic variant in CTNNB1/ $\beta$ -catenin as a novel cause for osteopathia striata with cranial sclerosis. *The Journal Of Clinical Endocrinology & Metabolism*. doi:10.1210/clinem/dgad757

Version: Publisher's Version

License: [Licensed under Article 25fa Copyright Act/Law \(Amendment Taverne\)](#)

Downloaded from: <https://hdl.handle.net/1887/3721117>

**Note:** To cite this publication please use the final published version (if applicable).

# A Mosaic Variant in *CTNNB1*/β-catenin as a Novel Cause for Osteopathia Striata With Cranial Sclerosis

Yentl Huybrechts,<sup>1</sup>  Natasha M. Appelman-Dijkstra,<sup>2</sup>  Ellen Steenackers,<sup>1</sup> Wouter Van Beylen,<sup>1</sup> Geert Mortier,<sup>1,3,4</sup>  Gretl Hendrickx,<sup>1,3,\*</sup>  and Wim Van Hul<sup>1,\*</sup> 

<sup>1</sup>Center of Medical Genetics, University of Antwerp and Antwerp University Hospital, 2650 Edegem, Belgium

<sup>2</sup>Department of Internal Medicine, Division Endocrinology, Leiden University Medical Center, 2300 Leiden, The Netherlands

<sup>3</sup>Laboratory for Skeletal Dysplasia Research, Department of Human Genetics, KU Leuven, 3000 Leuven, Belgium

<sup>4</sup>Center for Human Genetics, University Hospital Leuven, 3000 Leuven, Belgium

**Correspondence:** Wim Van Hul, PhD, Center of Medical Genetics, University of Antwerp and Antwerp University Hospital, Prins Boudewijnlaan 43, 2650 Edegem, Belgium. Email: [wim.vanhul@uantwerpen.be](mailto:wim.vanhul@uantwerpen.be).

\*These authors contributed equally to this study.

## Abstract

**Context:** Osteopathia striata with cranial sclerosis (OSCS) is a rare bone disorder with X-linked dominant inheritance, characterized by a generalized hyperostosis in the skull and long bones and typical metaphyseal striations in the long bones. So far, loss-of-function variants in *AMER1* (also known as *WTX* or *FAM123B*), encoding the APC membrane recruitment protein 1 (*AMER1*), have been described as the only molecular cause for OSCS. *AMER1* promotes the degradation of β-catenin via AXIN stabilization, acting as a negative regulator of the WNT/β-catenin signaling pathway, a central pathway in bone formation.

**Objective:** In this study, we describe a Dutch adult woman with an OSCS-like phenotype, namely, generalized high bone mass and characteristic metaphyseal striations, but no genetic variant affecting *AMER1*.

**Results:** Whole exome sequencing led to the identification of a mosaic missense variant (c.876A > C; p.Lys292Asn) in *CTNNB1*, coding for β-catenin. The variant disrupts an amino acid known to be crucial for interaction with AXIN, a key factor in the β-catenin destruction complex. Western blotting experiments demonstrate that the p.Lys292Asn variant does not significantly affect the β-catenin phosphorylation status, and hence stability in the cytoplasm. Additionally, luciferase reporter assays were performed to investigate the effect of p.Lys292Asn β-catenin on canonical WNT signaling. These studies indicate an average 70-fold increase in canonical WNT signaling activity by p.Lys292Asn β-catenin.

**Conclusion:** In conclusion, this study indicates that somatic variants in the *CTNNB1* gene could explain the pathogenesis of unsolved cases of osteopathia striata.

**Key Words:** high bone mass, canonical WNT signaling, *AMER1*, osteopathia striata with cranial sclerosis, *CTNNB1*, β-catenin

**Abbreviations:** *AMER1*, adenomatous polyposis coli (APC) membrane recruitment protein 1; *APC*, adenomatous polyposis coli; *CK1*, casein kinase 1; *CT*, computed tomography; *GSK3β*, glycogen synthase kinase 3β; *MRI*, magnetic resonance imaging; *OSCS*, osteopathia striata with cranial sclerosis; *WES*, whole exome sequencing.

Osteopathia striata with cranial sclerosis (OSCS, OMIM #300373) is a rare bone disorder, characterized by a generalized hyperostosis, affecting both the long bones and the skull, and the presence of characteristic metaphyseal striations in the pelvis and the long bones (1, 2). The majority of patients present with macrocephaly, cleft palate, hearing impairment, and typical facial features, such as frontal bossing and a broad nasal bridge. Up to 30% of patients experience (mild) developmental delay or cardiac abnormalities. OSCS is currently known to be inherited in an X-linked dominant manner, and males usually show a more severe phenotype compared to female patients. In 2009, Jenkins et al identified loss-of-function pathogenic variants in *AMER1* (previously known as *WTX* or *FAM123B*) as the genetic cause for OSCS (3). Although somatic mosaicism for *AMER1* pathogenic variants has been frequently reported in mildly affected male individuals, germline pathogenic variants

have also been described. The latter often do not result in the development of metaphyseal striations. Male individuals with a severe phenotype typically have multiple congenital malformations leading to fetal or neonatal death (1, 4–7).

*AMER1* encodes the adenomatous polyposis coli (APC) membrane recruitment protein 1 (*AMER1*), an important intracellular inhibitor of the β-catenin-dependent or canonical WNT signaling pathway, which is well-known in the context of sclerosing bone disorders (8, 9). The pathway is activated upon binding of a WNT ligand to the Frizzled-LRP5/6 receptor complex, allowing β-catenin to stabilize and accumulate in the cytoplasm, and translocate to the nucleus (Fig. 1). Here, it binds to TCF/LEF transcription factors to initiate the transcription of target genes, which in the context of bone tissue, contributes to bone formation by the osteoblasts. However, in the case of inactivity or inhibition of the canonical pathway,

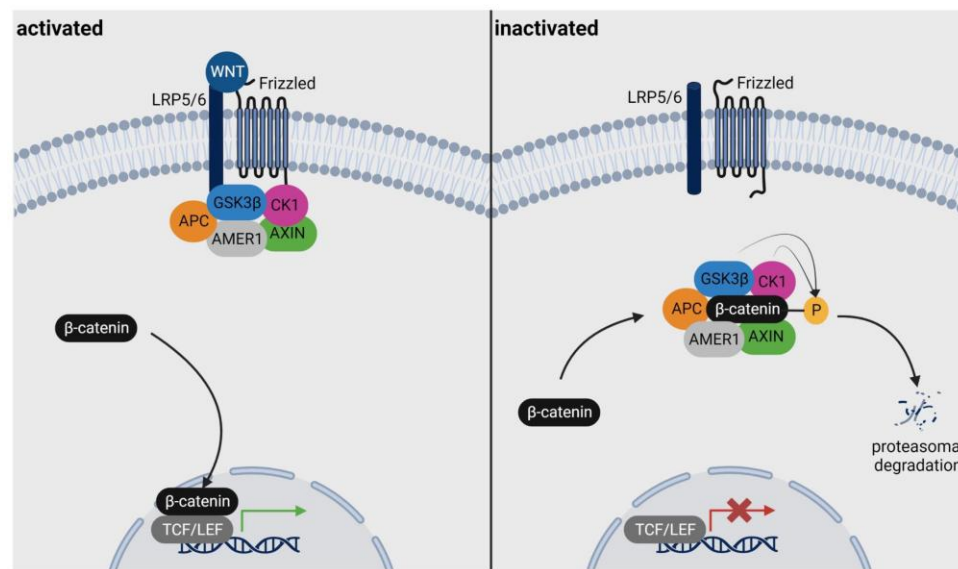


**Figure 1.** Canonical WNT signaling pathway. In the presence of WNT ligand (left panel), the destruction complex—consisting of adenomatous polyposis coli protein (APC), glycogen synthase kinase 3 $\beta$  (GSK3 $\beta$ ), casein kinase 1 (CK1), APC membrane recruitment protein 1 (AMER1), and AXIN—is inactivated, so that  $\beta$ -catenin can translocate to the nucleus, in which it initiates the transcription of target genes, which contributes to bone formation by osteoblasts. In the absence of WNT ligand (right panel), the destruction complex is active, resulting in phosphorylation and subsequent proteasomal degradation of  $\beta$ -catenin, and inhibition of the transcription of target genes.

$\beta$ -catenin binds to the destruction complex. This cytoplasmic protein complex consists of casein kinase 1 (CK1), glycogen synthase kinase 3 $\beta$  (GSK3 $\beta$ ), APC, and AXIN. Upon binding, the N-terminus of  $\beta$ -catenin is sequentially phosphorylated by CK1 and GSK3 $\beta$ , labeling it for subsequent proteasomal degradation, thereby preventing or inhibiting the transcription of target genes (10, 11) (Fig. 1).

AMER1 has a dual inhibitory function on canonical WNT signaling activity (12, 13). On the one hand, a direct interaction with different components of the  $\beta$ -catenin destruction complex—specifically,  $\beta$ -catenin, APC, and AXIN—has been reported (13-15). Using its phosphatidylinositol (4, 5)-bispophosphate-binding domains, AMER1 promotes the translocation of the destruction complex to the plasma membrane, hence facilitating the ubiquitination and proteasomal degradation of  $\beta$ -catenin (13, 16). On the other hand, it was demonstrated that AMER1 is involved in the stabilization of AXIN (13). It is suspected that the latter is the limiting component in  $\beta$ -catenin degradation and that AMER1 maintains its expression levels, thus counteracting Wnt-induced destabilization of AXIN (13, 17). Based on current findings, it is thus not unexpected that loss-of-function variants in *AMER1* are involved in the development of the high bone mass phenotype in OSCS patients.

In this study, we investigated an adult female individual with an OSCS phenotype, in whom no pathogenic variants in *AMER1* were identified. In order to unravel the underlying genetic cause, whole exome sequencing (WES) was performed, which led to the identification of a pathogenic mosaic variant in *CTNNB1*, encoding  $\beta$ -catenin. Finally, further functional studies were performed to assess the effect of the identified variant on the stabilization of  $\beta$ -catenin and on canonical WNT signaling activity. Here, we showed a strong induction of canonical WNT signaling activity by mutant  $\beta$ -catenin. This study therefore demonstrates that a mosaic gain-of-function variant in *CTNNB1*/ $\beta$ -catenin can cause a high bone mass phenotype of OSCS.

## Materials and Methods

### Study Subject

The subject is an adult woman originating from The Netherlands, from whom informed consent was obtained. Our study was conducted according to the World Medical Association Declaration of Helsinki on ethical principles for medical research involving human subjects (18) and approved by the Institutional Review Board (or Ethics Committee) of the University of Antwerp (B300201521651, 04/08/2014). Clinical assessment of the subject consisted of a radiographic examination (long bones, hands, skull, pelvis), magnetic resonance imaging (MRI) (vertebral column, skull), computed tomography (CT) (skull) and 2 dual-energy x-ray absorptiometry scans performed 3 years apart. Blood was drawn for the quantification of serum markers (calcium, phosphate, alkaline phosphatase, creatinine, sodium, potassium, magnesium, vitamin D, parathyroid hormone, C-terminal telopeptide of type I collagen (beta crosslaps, CTx, bone resorption marker), and procollagen type I N-propeptide (PINP, bone formation marker). Genomic DNA was isolated from peripheral blood of the patient.

### Genetic Analysis

Based on the suspected diagnosis of OSCS, as a first step, the coding regions of the *AMER1* gene were screened for putative pathogenic variants using Sanger sequencing as described previously (2). Given the normal results, whole exome sequencing was performed as a next step. Library preparation was carried out using the TruSeq Exome Library Prep Kit (Illumina), followed by sequencing using the “sequencing by synthesis” technology (Illumina). Initially, variant filtering was performed with VariantDB software in a large set of genes known to be associated with skeletal dysplasias (WESSD\_panel) (19). In addition, genome-wide Human Phenotype Ontology (HPO)-based filtering (MOON software, Invitae) was performed. A minimal coverage of 20 $\times$  for at least 90% of the target regions of the

WESSD gene panel was obtained. The WES data confirmed the absence of genetic variation in *AMER1*. Next, a variant of interest in exon 6 of *CTNNB1* (c.876A>C, transcript ENST00000349496.11, hg38) was confirmed with Sanger sequencing using 3 different primer sets (positions and sequences available upon request). MutationTaster (20), the combined annotation dependent depletion (CADD) score (21), SIFT (22), and PolyPhen-2 (23) were used to assess the pathogenic potential of the variants in silico.

### Expression Constructs and In Vitro Mutagenesis

The c.876A>C variant was introduced in a wild-type full-length human *CTNNB1* expression construct (transcript variant 1, NM\_001904, #SC107921, OriGene Technologies) using the Q5 Site-Directed Mutagenesis Kit (BioLabs). Sanger sequencing was used to verify the complete insert for the presence of the variant of interest and the absence of PCR errors.

### Western Blot

For the Western blot experiments,  $7 \times 10^5$  HEK293T cells/well were plated in 6-well plates. Twenty-four hours later, cells were transfected with wild-type or mutant *CTNNB1* construct (3000 ng) using FuGene6 (Promega) according to the manufacturer's protocol. The next day, serum-free DMEM was added to the cells and 6 hours later, cells were lysed using radioimmunoprecipitation assay (RIPA) buffer (Thermo Fischer Scientific), supplemented with protease (cOmplete™, EDTA-free Protease Inhibitor Cocktail, Roche) and phosphatase (PhosSTOP™, Roche) inhibitors. Equal amounts (20 µg) were loaded on a 4%-12% Bis-Tris Midi Gel (Invitrogen) and proteins were then transferred to a nitrocellulose membrane. Blocking was carried out in 5% bovine serum albumin (BSA) and 0.1% TBST (Tris-buffered saline with 0.1% Tween®20 Detergent), followed by overnight incubation at 4 °C with a primary antibody against (phospho-)β-catenin (Cell Signaling Technology #9562 [RRID: AB\_331149], 1:2000 or #9561 [RRID: AB\_331729], 1:1000) and subsequent probing with a secondary goat anti-rabbit antibody (Bio-Rad Cat# 170-6515 [RRID: AB\_11125142]), conjugated with horseradish peroxidase (1:10 000). Anti-β-actin (Sigma-Aldrich Cat# A5316 [RRID: AB\_476743]) was included to normalize for the amount of protein loaded and 3 independent experiments were performed. The amount of total and phosphorylated β-catenin, wild-type vs mutant, was statistically compared using Student *t* tests (GraphPad Prism 9).

### Luciferase Reporter Assay

HEK293T cells were plated at  $3 \times 10^4$  cells/well in 96-well plates. Upon approximately 70% confluency, co-transfection of TOPflash (20 ng) and pRL-TK (2 ng) plasmids with either wild-type or mutant *CTNNB1* (2.5 ng or 5 ng) was performed using FuGene6 (Promega). In addition, WNT1-V5 (2 ng), mesdc-2 (2 ng), and LRP5 (2 ng) were co-transfected to stimulate the canonical WNT signaling pathway. When needed, empty pcDNA3.1 vector was added to make the total DNA amount equal for all transfection experiments. Forty-eight hours after transfection, luciferase activity was measured using the Dual-Luciferase Reporter Assay System (Promega Corporation) on the Glomax Multi+ Luminometer (Promega Corporation). Three separate experiments were performed and ratios of the firefly and renilla luciferase measurements were expressed as relative to a negative control (empty vector

and luciferases). The different conditions were statistically compared using Student *t* tests (GraphPad Prism 9).

## Results

### Clinical Description

The proband is a 46-year-old Dutch woman presenting with headaches for clinical assessment. She has 4 healthy siblings and a twin sibling who died during pregnancy (Fig. 2A). She also has a 22-year-old son, who reportedly had learning difficulties as a child. Her adult height is 166 cm (−0.6 SD) and her weight is 52 kilograms. Her head circumference is 58 cm (+2 SD). She shows a facial dysmorphism, as evidenced by a broad, high nasal bridge, wide-set eyes, and a large mouth. Dental abnormalities, short toes, and an abnormally low-pitched voice were also observed. Although not further examined, moderate intellectual disability was suspected.

Radiographic examination showed hyperostosis of the long bones, the pelvis, the spine, and the skull (Fig. 2C-2F). Dual-energy x-ray absorptiometry measurements demonstrated a highly increased bone mineral density of the left femoral neck (FN-BMD, T-score: +7). Linear striations were observed at the metaphyses of humerus, femur, and proximal tibiae (Fig. 2C and 2D). MRI of the skull showed intracranial ossification of the tentorium edge, abnormal bone of the skull with thickening of the corticomodullary differentiation, and increased bone density in the upper jaw, the sphenoid bone, and zygoma. MRI of the vertebral column also demonstrated sclerotic margins of the vertebral corpora. A CT of the skull demonstrated denser facial bones and temporal bone, as well as an abnormal course of the facial nerve and anomalies of the inner ear. Furthermore, unilateral choanal atresia, hearing impairment, and retinal coloboma were reported. The proband also has abnormalities of the left hand with cutaneous syndactyly of the third and fourth fingers and preaxial polydactyly (extra thumb).

There is no evidence or history of tumors in the proband. Serum levels of (albumin-corrected) calcium, phosphate, alkaline phosphatase, sodium, potassium, and magnesium were all within normal reference ranges. Biochemical analysis showed no renal abnormalities (eGFR > 90 mL/min/1.73 m<sup>2</sup>). Over the past 6 years, the proband's symptoms did not worsen, nor were there signs of malignancies.

### Genetic Analysis of the Proband

Based on the clinical suspicion of OSCS, genetic screening of *AMER1* was carried out, but did not result in the identification of pathogenic variants. For this reason, whole exome sequencing was performed which revealed low level mosaicism for a missense variant in exon 6 of *CTNNB1* (c.876A>C) predicted to substitute Lys at position 292 into Asn (Fig. 3A and 3B). The p.Lys292Asn variant is located in the fourth Armadillo repeat of the encoded β-catenin protein (Fig. 3C). This variant is not listed in the gnomAD (26) or dbSNP databases, neither in heterozygous nor in homozygous state. The c.876A>C variant has a combined annotation dependent depletion (CADD) score of 23.6 and in silico predictions by PolyPhen-2 and MutationTaster categorizes the variant as “probably damaging” (score of 0.981) and “disease causing” (score of 0.84), respectively.

Interestingly, based on our exome data, a total of 82 reads were obtained at the level of our variant, of which 24% (n = 20) carried the c.876A>C alteration (IGV, version

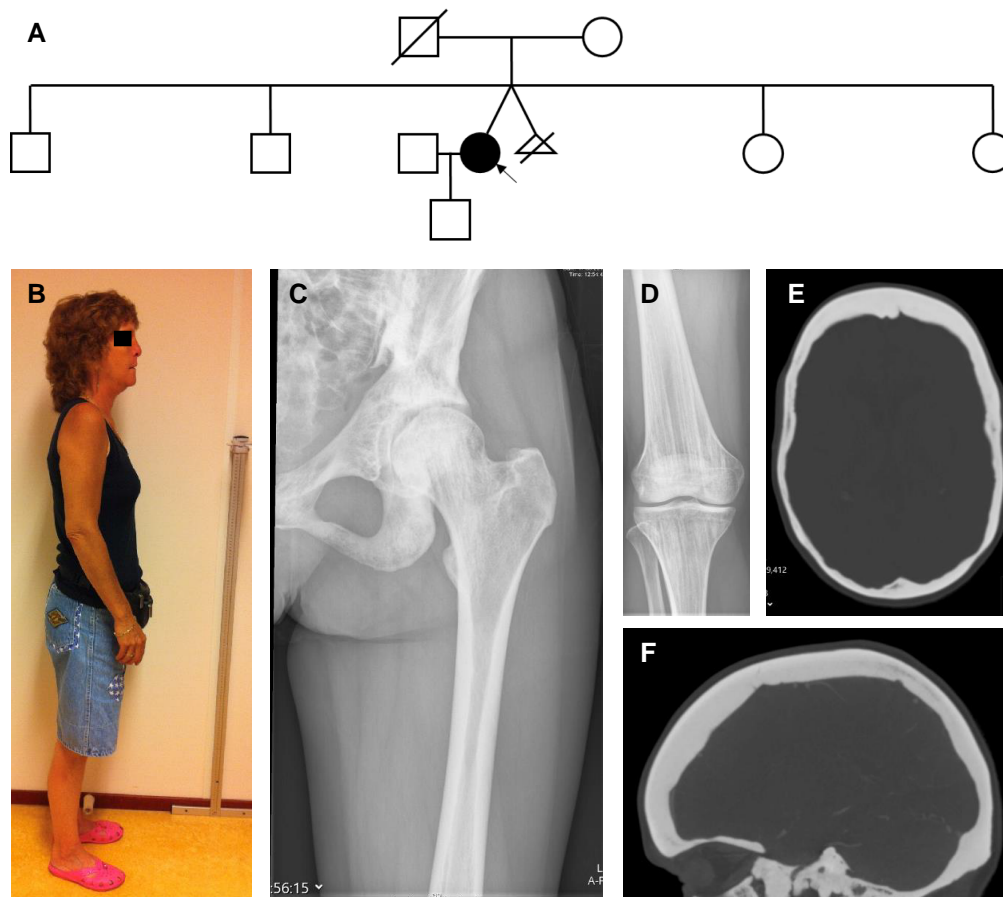


**Figure 2.** Clinical and radiographic features of the proband. (A) Pedigree of the family. (B) Profile view of the proband. Note the high nasal bridge. (C, D) Radiograph of the pelvis, proximal part of the femur and right knee shows patchy hyperostosis in the femoral head, acetabular roof, and distal part of the iliac wing, a thickened cortex of the femur diaphysis and metaphyseal linear striations in the femoral neck and knee. (E, F) Skull radiographs demonstrate hyperostosis of the cranial vault.

2.15.4). As this is significantly lower than the theoretically expected 50% altered alleles for a heterozygous variant ( $P = .0011$ , Fisher exact test), it is strongly indicated that the variant is mosaic in our patient. In line with this observation, direct Sanger sequencing of the region surrounding the c.876A > C variant in *CTNNB1*, confirmed the presence of the variant, although peak height was lower than seen for a regular heterozygous variant in both the forward and the reverse sequence (Fig. 3B). Using QSVAnalyzer software (27), it was demonstrated that the peak height of the altered allele was 10% and 23% for the reverse and forward sequences, respectively, which is in line with our WES data. Moreover, a similar result was obtained by amplification and Sanger sequencing of the chromosomal region of interest, using 2 additional primer sets (data not shown). Unfortunately, absence of the *CTNNB1* variant could not be confirmed in the proband's parents, siblings, or son, as no DNA was available from these relatives.

### Functional Evaluation of the p.Lys292Asn Variant in $\beta$ -catenin

To investigate the functional impact of the p.Lys292Asn variant, we first determined whether the identified variant affects the activity of  $\beta$ -catenin at the level of its stability in the cytoplasm. This was done by determining the phosphorylation status of the Ser33/37/Thr41 residues of  $\beta$ -catenin, labeling  $\beta$ -catenin for proteasomal degradation when phosphorylated by GSK3 $\beta$ .

Western blotting and quantification of total and phosphorylated  $\beta$ -catenin did not support an effect of the p.Lys292Asn variant on stabilization of  $\beta$ -catenin. This was shown by the similar ratios of phosphorylated  $\beta$ -catenin over the total amount of  $\beta$ -catenin for wild-type vs mutant  $\beta$ -catenin ( $P = .21$ ; Fig. 4A and 4B).

In our next step, the effect of the p.Lys292Asn variant on the canonical WNT signaling activity was investigated, as  $\beta$ -catenin plays a pivotal role in its activation. Using luciferase reporter assays (TOPflash) in HEK293T cells, it was shown that overexpression of 2 different amounts of mutant *CTNNB1* results in a dose-dependent 60-fold to 80-fold increase in canonical WNT signaling activity, compared to overexpression of equal amounts of wild-type *CTNNB1* (Fig. 4C). Taken together, these functional results demonstrate a gain-of-function effect of the p.Lys292Asn  $\beta$ -catenin variant on canonical WNT signaling.

### Discussion

In this study, we report on a 46-year-old Dutch woman with phenotypic features that strongly resemble OSCS (Table 1). She presented with hyperostosis of the long bones, the pelvis, the spine and the skull, and linear striations were observed at the metaphyses of humerus, femur, and proximal tibia. As for our subject, additional OSCS features were reported, including macrocephaly, dental abnormalities, hearing loss, and a broad nasal bridge. Interestingly, the proband also presented with

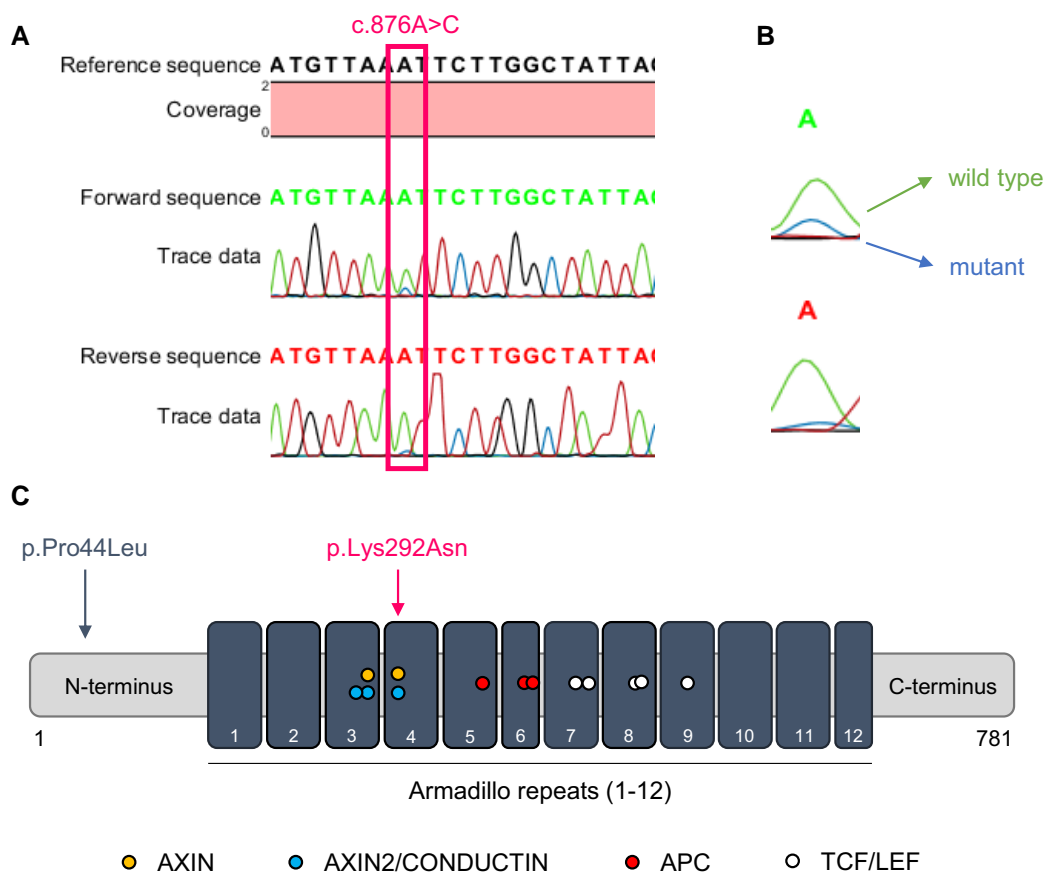


**Figure 3.** (A) Identification of a de novo mosaic c.876A > C variant in *CTNNB1* in the proband. (B) Magnification of the sequence showing the mosaic c.876A > C variant. The wild-type and mutant sequence tracks are indicated with arrows. Two additional amplifications with different primer sets resulted in similar results (C) Schematic overview of the  $\beta$ -catenin protein structure and location of the previously reported p.Pro44Leu variant (24) and the p.Lys292Asn variant, identified in the current study. Amino acids previously reported as hot spots for binding with AXIN, AXIN2/Conductin, APC, and TCF/LEF are indicated with specific colors (25).

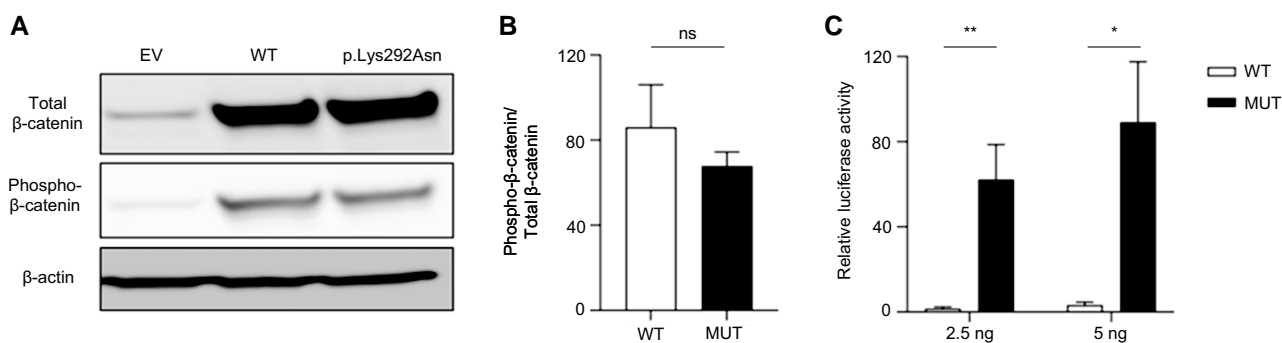


**Figure 4.** Impact of the p.Lys292Asn variant on the  $\beta$ -catenin phosphorylation status and WNT/ $\beta$ -catenin signaling activity. (A, B) Western blot experiments in HEK293T cells show no effect of the p.Lys292Asn variant on phosphorylation of  $\beta$ -catenin at the Ser33/37/Thr41 amino acid residues. Levels of (phospho-) $\beta$ -catenin were normalized for total amount of protein using  $\beta$ -actin levels (in %). (C) TOPflash luciferase reporter assays in HEK293T cells demonstrate that overexpression of mutant  $\beta$ -catenin results in significantly higher relative luciferase activity compared to wild-type  $\beta$ -catenin. Ratios of firefly and renilla measurements are expressed as relative to a negative control. Data are represented as mean  $\pm$  SD and statistical testing is carried out using Student *t* tests. Abbreviation: ns, not significant; \*  $P < .05$ ; \*\*  $P < .01$ .

polysyndactyly, which has been described in some severely affected male cases with OSCS (3, 5). Overall, the clinical and radiographic findings suggest that the proband in our study presents with a skeletal bone disorder reminiscent of *AMER1*-related OSCS (Table 1).

Because of the genomic location of *AMER1*, OSCS has an X-linked mode of inheritance. The proband in our study tested negative for pathogenic variants in *AMER1* and whole exome

sequencing led to the identification of a somatic, mosaic pathogenic variant in *CTNNB1*. The mosaic status of the variant is supported by the allele ratio in the WES data (24% mutant) and the fact that a similar ratio was obtained in 3 independent Sanger sequencing experiments. Interestingly, the metaphyseal striations observed in *AMER1*-related OSCS are due to mosaicism in male subjects, or by Lyonization in female subjects. Unfortunately, no DNA material is available to further

**Table 1. Clinical and genetic characteristics of individuals with  $\beta$ -catenin or AMER1 variants**

	$\beta$ -catenin (p.Lys292Asn)	$\beta$ -catenin (p.Pro44Leu) (24)	AMER1 (p.Arg358X) (2)	AMER1 (p.Gln335X) (28)
Diagnosis	OSCS	Osteosclerosis	OSCS	OSCS
Inheritance	NA	De novo	X-linked dominant	X-linked dominant
Mosaicism	+ (somatic)	–	+ (X-inactivation)	+ (X-inactivation)
Mutation effect	Gain-of-function	Gain-of-function	Loss-of-function	Loss-of-function
Facial features				
Eyes	Wide-set	Wide-set	Deep-set	Wide-set
Nasal bridge	Broad, high	Depressed	Broad	Broad, depressed
Cleft palate	–	+	+	–
Ears	NA	Low-set	NA	Low-set
Macrocephaly	+	+	+	+
Intellectual disability	+/-	–	–	–
Hearing impairment	+	NA	+	+
Dental abnormalities	+	–	–	+
Height	Normal	75th percentile	0.4th percentile	25th percentile
Hyperostosis				
Skull	+	+	+	+
Long bones	+	+	+	+
Pelvis	+	+	+	+
Syn-/polydactyly	+	–	–	–
Metaphyseal striations	+	–	+	+
Neoplasia	–	+ (adrenocortical)	–	+ (pituitary macroadenoma)
Other	Retinal coloboma	Virilization	Cardiac anomaly	NA

This table compares the phenotype of *CTNNB1*-mutated subjects to the phenotype of randomly selected *AMER1* cases. Abbreviations: NA, not available; OSCS, osteopathia striata with cranial sclerosis.

investigate if the son also has the variant. However, we consider the chance that the son is a heterozygous carrier of the variant small, as one would expect a more severe phenotype if this was the case.

*CTNNB1* encodes  $\beta$ -catenin, a key regulator of the WNT/ $\beta$ -catenin or canonical WNT pathway, which is indispensable in bone formation (29-32). However, until recently, genetic variation in *CTNNB1* was mainly associated with nonskeletal phenotypes. Somatic gain-of-function variants in *CTNNB1* have been linked to a variety of cancers, including colorectal and ovarian cancer (33-35). Furthermore, germline heterozygous loss-of-function variants have been described to be causative for neurodevelopmental disorder with spastic diplegia and visual defects (OMIM #615075) and to be associated with intellectual disability and autism spectrum disorder (36-40). Given its major importance in canonical WNT signaling and bone biology, it is surprising that the first disease-causing variant in *CTNNB1* in a (sclerosing) skeletal dysplasia was only reported in 2020 by Peng and colleagues (Table 1) (24). In their study, the authors identified a de novo variant (c.131C > T; p.Pro44Leu) at the N-terminus of  $\beta$ -catenin in a girl with hyperostosis of the long bones, pelvis, and skull. Interestingly however, no metaphyseal striations could be observed in the pelvis or long bones of this case. The p.Pro44Leu variant is located at the N-terminus of  $\beta$ -catenin and affects the threonine/serine residues that are phosphorylated by GSK-3 $\beta$  to initiate proteasomal degradation (41, 42). Hence, impaired phosphorylation results in the stabilization of the protein and increased canonical WNT signaling activity (24, 41-43). In addition, the patient presented with an adrenocortical adenoma. This could

be attributed to a location-specific effect, as the variant is located in the third exon, where an increased frequency of variants has also been observed in various cancer types (34). However, since somatic variants in cancer do not occur exclusively in exon 3, the development of a malignancy in our proband cannot be ruled out, which is why strict monitoring is recommended.

Due to the remarkable overlap between the phenotypes of our subject and the *AMER1*-related OSCS cases, it can be hypothesized that a similar underlying mechanism must be involved in the pathogenesis. It is generally thought that the main purpose of the  $\beta$ -catenin destruction complex is to bring  $\beta$ -catenin in close proximity to the kinases (CK1 and GSK3 $\beta$ ) in order to facilitate phosphorylation (13). An essential, yet limiting, component of this protein complex is AXIN, which serves as a scaffold protein (44). Currently, it is clear that changes in AXIN levels directly lead to alterations in canonical WNT signaling activity, and maintaining these AXIN levels and thus suppressing WNT signaling is a crucial task of *AMER1* (13, 17). Furthermore, Fagotto and colleagues demonstrated that  $\beta$ -catenin-binding sites are essential for proper function of AXIN (45). According to a previous study, the p.Lys292Asn variant is located in a so-called “hot spot” for interaction with AXIN (25). In their extensive study, Von Kries et al mutated exactly the Lys292 residue and showed subsequent defective binding with AXIN, using alanine scanning and subsequent yeast two-hybrid analysis. Eventually, it was demonstrated that the Lys292  $\beta$ -catenin mutant was resistant to degradation. Hence, this supports our hypothesis that the p.Lys292Asn variant in  $\beta$ -catenin prevents degradation of the protein, leading to increased WNT signaling

activity and the sclerosing bone phenotype in the proband. Given the complexity of the destruction complex and the canonical WNT signaling pathway in general, it is challenging to draw a clear-cut conclusion regarding the exact underlying pathological mechanism. However, although further research into stabilization of  $\beta$ -catenin would be of interest, we can reasonably expect, based on current knowledge, that disrupted axin binding (at least partially) contributes to the development of the phenotype.

In conclusion, we report the identification of a novel mosaic p.Lys292Asn variant in  $\beta$ -catenin in an adult female with a phenotype that shares clinical and radiographic features with OSCS. Until now, the striations phenotype in classical OSCS has been linked to the mechanism of X-inactivation as a pathogenic mechanism. However, our findings add somatic variants as a possible cause. Furthermore, it implies that impaired  $\beta$ -catenin-AXIN binding can be identified as a disease-causing mechanism for a high bone mass disorder. The identification of the mosaic p.Lys292Asn variant expands the mutational spectrum of  $\beta$ -catenin-related (bone) disorders, which is of major importance for better understanding the role of  $\beta$ -catenin in various processes, as well as for future diagnostic testing of individuals affected with an OSCS-like phenotype.

## Funding

This research was funded by a research grant of the University of Antwerp (Methusalem—OEC grant—“GENOMED”; FFB190208) and the UZA foundations (21MGN04, Siebe Van Reusel Fonds).

## Disclosures

The authors have nothing to disclose.

## Data Availability

Data sharing is not applicable to this article as no datasets were generated or analyzed during the current study.

## References

- Gear R, Savarirayan R. Osteopathia striata with cranial sclerosis. In: Adam MP, Feldman J, Mirzaa GM, *et al.*, eds. *GeneReviews*® [Internet]. University of Washington; 2021:1993-2024.
- Perdu B, de Freitas F, Frints SG, *et al.* Osteopathia striata with cranial sclerosis owing to WTX gene defect. *J Bone Miner Res.* 2010;25(1):82-90.
- Jenkins ZA, van Kogelenberg M, Morgan T, *et al.* Germline mutations in WTX cause a sclerosing skeletal dysplasia but do not predispose to tumorigenesis. *Nat Genet.* 2009;41(1):95-100.
- Perdu B, Lakeman P, Mortier G, Koenig R, Lachmeijer AM, Van Hul W. Two novel WTX mutations underscore the unpredictability of male survival in osteopathia striata with cranial sclerosis. *Clin Genet.* 2011;80(4):383-388.
- Holman SK, Daniel P, Jenkins ZA, *et al.* The male phenotype in osteopathia striata congenita with cranial sclerosis. *Am J Med Genet A.* 2011;155(10):2397-2408.
- Joseph DJ, Ichikawa S, Econs MJ. Mosaicism in osteopathia striata with cranial sclerosis. *J Clin Endocrinol Metab.* 2010;95(4):1506-1507.
- Rott H, Krieg P, Rüttschle H, Kraus C. Multiple malformations in a male and maternal osteopathia striata with cranial sclerosis (OSCS). *Genet Couns.* 2003;14(3):281-288.
- Huybrechts Y, Mortier G, Boudin E, Van Hul W. WNT signaling and bone: lessons from skeletal dysplasias and disorders. *Front Endocrinol (Lausanne).* 2020;11:165.

- Bergen DJ, Maurizi A, Formosa MM, *et al.* High bone mass disorders: new insights from connecting the clinic and the bench. *J Bone Miner Res.* 2023;38(2):229-247.
- Stamos JL, Weis WI. The  $\beta$ -catenin destruction complex. *Cold Spring Harb Perspect Biol.* 2013;5(1):a007898.
- Kim N-G, Xu C, Gumbiner BM. Identification of targets of the Wnt pathway destruction complex in addition to  $\beta$ -catenin. *Proc Natl Acad Sci U S A.* 2009;106(13):5165-5170.
- Große A, Perner B, Naumann U, Englert C. Zebrafish Wtx is a negative regulator of Wnt signaling but is dispensable for embryonic development and organ homeostasis. *Dev Dyn.* 2019;248(9):866-881.
- Tanneberger K, Pfister AS, Kriz V, Bryja V, Schambony A, Behrens J. Structural and functional characterization of the Wnt inhibitor APC membrane recruitment 1 (Amer1). *J Biol Chem.* 2011;286(22):19204-19214.
- Major MB, Camp ND, Berndt JD, *et al.* Wilms tumor suppressor WTX negatively regulates WNT/ $\beta$ -catenin signaling. *Science.* 2007;316(5827):1043-1046.
- Mi J, Parthasarathy P, Halliday BJ, *et al.* Deletion of exon 1 in AMER1 in osteopathia striata with cranial sclerosis. *Genes (Basel).* 2020;11(12):1439.
- Grohmann A, Tanneberger K, Alzner A, Schneikert J, Behrens J. AMER1 regulates the distribution of the tumor suppressor APC between microtubules and the plasma membrane. *J Cell Sci.* 2007;120(21):3738-3747.
- Lee E, Salic A, Krüger R, Heinrich R, Kirschner MW. The roles of APC and axin derived from experimental and theoretical analysis of the Wnt pathway. *PLoS Biol.* 2003;1(1):E10.
- Association WM. World Medical Association Declaration of Helsinki: ethical principles for medical research involving human subjects. *JAMA.* 2013;310(20):2191-2194.
- Vandeweyer G, Van Laer L, Loeys B, Van den Bulcke T, Kooy RF. VariantDB: a flexible annotation and filtering portal for next generation sequencing data. *Genome Med.* 2014;6(10):74.
- Steinhaus R, Proft S, Schuelke M, Cooper DN, Schwarz JM, Seelow D. MutationTaster2021. *Nucleic Acids Res.* 2021;49(W1):W446-W451.
- Kircher M, Witten DM, Jain P, O’Roak BJ, Cooper GM, Shendure J. A general framework for estimating the relative pathogenicity of human genetic variants. *Nat Genet.* 2014;46(3):310-315.
- Ng PC, Henikoff S. SIFT: predicting amino acid changes that affect protein function. *Nucleic Acids Res.* 2003;31(13):3812-3814.
- Adzhubei I, Jordan DM, Sunyaev SR. Predicting functional effect of human missense mutations using PolyPhen-2. *Curr Protoc Hum Genet.* 2013;Chapter 7:Unit7.20.
- Peng H, Jenkins ZA, White R, *et al.* An activating variant in CTNBN1 is associated with a sclerosing bone dysplasia and adrenocortical neoplasia. *J Clin Endocrinol Metab.* 2020;105(3):688-695.
- von Kries JP, Winbeck G, Asbrand C, *et al.* Hot spots in  $\beta$ -catenin for interactions with LEF-1, conductin and APC. *Nat Struct Biol.* 2000;7(9):800-807.
- Karczewski KJ, Francioli LC, Tiao G, *et al.* The mutational constraint spectrum quantified from variation in 141,456 humans. *Nature.* 2020;581(7809):434-443.
- Carr IM, Robinson JI, Dimitriou R, Markham AF, Morgan AW, Bonthron DT. Inferring relative proportions of DNA variants from sequencing electropherograms. *Bioinformatics.* 2009;25(24):3244-3250.
- Jeong C, Kim M, Yim J, Park I-J, Lee J, Lee J. Novel WTX nonsense mutation in a family diagnosed with osteopathia striata with cranial sclerosis: case report. *Medicine (Baltimore).* 2021;100(40):e27346.
- Duan P, Bonewald L. The role of the wnt/ $\beta$ -catenin signaling pathway in formation and maintenance of bone and teeth. *Int J Biochem Cell Biol.* 2016;77(Pt A):23-29.
- Glass DA, Karsenty G. Canonical Wnt signaling in osteoblasts is required for osteoclast differentiation. *Ann N Y Acad Sci.* 2006;1068(1):117-130.
- Frigroryan T, Wend P, Klaus A, Birchmeier W. Deciphering the function of canonical Wnt signals in development and disease: conditional loss-and gain-of-function mutations of  $\beta$ -catenin in mice. *Genes Dev.* 2008;22(17):2308-2341.



32. Jia M, Chen S, Zhang B, Liang H, Feng J, Zong Z. Effects of constitutive  $\beta$ -catenin activation on vertebral bone growth and remodeling at different postnatal stages in mice. *PLoS One*. 2013;8(9):e74093.
33. Gao C, Wang Y, Broaddus R, Sun L, Xue F, Zhang W. Exon 3 mutations of CTNNB1 drive tumorigenesis: a review. *Oncotarget*. 2018;9(4):5492-5508.
34. Kim S, Jeong S. Mutation hotspots in the  $\beta$ -catenin gene: lessons from the human cancer genome databases. *Mol Cells*. 2019;42(1):8-16.
35. Liu P, Liang B, Liu M, *et al*. Oncogenic mutations in armadillo repeats 5 and 6 of  $\beta$ -catenin reduce binding to APC, increasing signaling and transcription of target genes. *Gastroenterology*. 2020;158(4):1029-1043.e10.
36. Kuechler A, Willemsen MH, Albrecht B, *et al*. De novo mutations in beta-catenin (CTNNB1) appear to be a frequent cause of intellectual disability: expanding the mutational and clinical spectrum. *Hum Genet*. 2015;134(1):97-109.
37. Kayumi S, Pérez-Jurado LA, Palomares M, *et al*. Genomic and phenotypic characterization of 404 individuals with neurodevelopmental disorders caused by CTNNB1 variants. *Genet Med*. 2022;24(11):2351-2366.
38. Lee S, Jang SS, Park S, *et al*. The extended clinical and genetic spectrum of CTNNB1-related neurodevelopmental disorder. *Front Pediatr*. 2022;10:960450.
39. Dubruc E, Putoux A, Labalme A, Rougeot C, Sanlaville D, Edery P. A new intellectual disability syndrome caused by CTNNB1 haploinsufficiency. *Am J Med Genet A*. 2014;164(6):1571-1575.
40. Kumar S, Reynolds K, Ji Y, Gu R, Rai S, Zhou CJ. Impaired neurodevelopmental pathways in autism spectrum disorder: a review of signaling mechanisms and crosstalk. *J Neurodev Disord*. 2019;11(1):10.
41. Shah K, Kazi JU. Phosphorylation-dependent regulation of WNT/ $\beta$ -catenin signaling. *Front Oncol*. 2022;12:858782.
42. Liu C, Li Y, Semenov M, *et al*. Control of  $\beta$ -catenin phosphorylation/degradation by a dual-kinase mechanism. *Cell*. 2002;108(6):837-847.
43. Dar MS, Singh P, Mir RA, Dar MJ.  $\beta$ -catenin N-terminal domain: an enigmatic region prone to cancer causing mutations. *Mutat Res Rev Mutat Res*. 2017;773:122-133.
44. Schaefer KN, Peifer M. Wnt/ $\beta$ -catenin signaling regulation and a role for biomolecular condensates. *Dev Cell*. 2019;48(4):429-444.
45. Fagotto F, Jho E-h, Zeng L, *et al*. Domains of axin involved in protein-protein interactions, Wnt pathway inhibition, and intracellular localization. *J Cell Biol*. 1999;145(4):741-756.